Applied mixture optimization techniques for paste design of bonded roller-compacted fibre reinforced polymer modified concrete (BRCFRPMC) overlays

Olubanwo, A. and Karadelis, J.N.

Applied Mixture Optimization Techniques for Paste Design of Bonded Roller-Compacted Fibre Reinforced Polymer Modified Concrete (BRCFRPMC) Overlays.

Adegoke Omotayo Olubanwo[1]
John Nicholas Karadelis[2]
Department of Civil Engineering, Architecture and Building, Coventry University, Priory Street, Coventry, United Kingdom, CV1 5FB.

[1] **Email: aa7878@coventry.ac.uk Tel: +44-02477659025**
[2] **Email: aa9118@coventry.ac.uk Tel: +44-02477658992**

Abstract

The overall composite performance of concrete is generally contingent on achieving the right proportion of blend. The use of mixture experiments provides a flexible, easy, and quick way of optimizing multi-component materials of this nature. This paper describes the use of optimization techniques within the concept of material mixture experiments for proportioning and designing the paste component of a Bonded Roller Compacted Fibre Reinforced Polymer Modified Concrete (BRCFRPMC). By constraining the range of variability of the paste constituents, a feasible design space was created with 13 experimental points treated based on the required structural and elastic properties of the overlay. The optimum consistency-time for full consolidation and composite behaviour with the substrate ordinary Portland cement concrete (OPCC) was established between 34.1 and 34.9 seconds, while the resulting apparent maximum density achieves between 97.1% - 98.0% of the theoretical air-free density. The tensile and shear interfacial tests performed on the optimum mixture overlay also exhibited good bonding capability with the substrate OPCC. The combined effects of curing age and surface texture on bonding were also underlined.

Keywords: Concrete; Mixture Experiments; Overlay; Optimization; BRCFRPMC; OPCC; Consolidation.

List of Abbreviations:

BRCFRPMC - Roller Compacted Fibre Reinforced Polymer Modified Concrete
RCC - Roller Compacted Concrete
OPCC – Ordinary Portland Cement Concrete
TAFD - Theoretical Air-Free Density
AMD – Apparent Maximum Density
MVB – Modified Vebe
PMC – Polymer Modified Concrete
EVD - Extreme-Vertices Design
SI – Solid Inclusions
P – Paste
ANOVA – Analysis of Variance

1.0. Introduction

In spite of the limited funding available for highway maintenance, the ageing highway pavement structures, and the increased heavy traffic loading, it is incumbent on the road maintenance agencies to ensure that prompt and expedited maintenance approaches are made available to meet the socio-economic needs of the road-users. These days, much of the effort among practitioners seeks mainly to promote repair materials and methods with low life-cycle costs, while ensuring quality is not compromised [1].

To a great extent, research works in areas of novel and advanced engineered materials seem to be providing headway, especially with the advent of new admixtures, additives, and high-speed computational tools. With new additives and admixtures, enhanced material properties are made possible; while with high-speed digital computers, many difficult-to-solve problems, particularly complex mixture optimization problems, can now be unravelled within the shortest possible time frame.

Although, applied optimization techniques are nearly as old as *calculus of variations*, their direct and possibly frequent application to mixture processing in concrete industry is still relatively new, compared to pharmaceutical, petrochemical, and medical biology where considerable successes have been recorded [2].

In concrete industry, the use of historical data or traditional trail-and-error mixture proportioning methods based on ACI 211.1 [3] is common, and has long enjoyed wider acceptance. However its applications can be rigorous and uneconomical, particularly where several material constituents and complex multi-criteria properties are involved. Besides, neither method gives a detailed procedure for optimizing mixtures [4], which at this point necessitates the need for a more robust and time / cost-effective method.

The use of mixture optimization techniques is now fast gaining acceptance among concrete experts. In the present study, a high performing Bonded Roller Compacted Fibre Reinforced Polymer Modified Concrete overlay (BRCFRPMC) is designed using Mixture Optimization Techniques to meet the following multi-criteria performance: (1) No sinking attribute during vibratory compaction, (2) sufficient mechanical and dimensional compatibility stability with the substrate, and (3) early and durable interfacial bond performance.

The overall objective is to ensure that the designed overlay material is optimized for both structural and composite performances. The corresponding benchmarks for performance output are given later in Table 13, while Figure 1 shows the flowchart diagram of the optimization process and the general methodical procedures followed in this work. The procedures involved:

1. Initial desirability goal setting (Identifying multi-criteria optimum responses of the mixture in its wet and dry states).
2. Mixture Model idealization (Phase classification - solid and paste phases)
3. Screening of components (Reducing component variable to paste constituents i.e. CEM1, SBR, WATER)
4. Mixture Model formulation (Initial trial mixes based on $[N(2)^{N-1}+1]$ possible combinations)
5. Mixture testing and characterization (Fresh and hardened states)
6. Individual desirability weighing and checking
7. Composite desirability weighing and checking
8. Overall Result verification
9. Interfacial Bonding (surface preparation, bonding, curing, and testing)
10. Bond reliability assessment

2.0 Material and Test Requirements of BRCFRPMC.

2.1 Roller Compacted Concrete Overlay

In ACI 207.5R [5], Roller Compacted Concrete (RCC) is defined as concrete compacted by a vibrating roller. RCC therefore differs from conventional concrete principally in its consistency requirement. For effective consolidation, the concrete mixture must be dry enough to prevent sinking of the vibratory roller equipment, but sufficiently wet to permit adequate distribution of the binder paste in the concrete during mixing. In addition, in situations where RCC is applied as a bonded overlay, it should as a necessity provide good bonding with the substrate [1].

In order to ensure proper mixture proportioning of RCC, ACI 207.5R [5] identifies five distinct methods, but in practice, only two main approaches are common.

The first approach is based on the principle of soil compaction, where the optimum water content of the concrete results in a mix with maximum compacted density. Typically, the best compaction is expected to yield the best strength; and that occurs only when the operating vibrating roller is effectively supported.

The second approach is based on the use of concrete consistency tests to produce a high-paste RCC mixture. In this method, mixture proportioning is dependent on achieving good consolidation, thereby ensuring that much of the void content is filled with paste, even at a considerable low water content.

In the present work, the latter was employed due to its associated high-paste content required for good bonding with the substrate. Besides, the apparent maximum density (AMD) in concrete consistency approach is normally greater than that of soil compaction approach. Typically its value can be as high as 98% of the theoretical air-free density (TAFD) [6].

Hence, for very stiff to extremely dry RCC mixtures like the present; the test samples were prepared with Modified-Vebe (MVB) method in accordance to ASTM C1170 / C1170M-08 requirements [7]. The vibration induced by the apparatus is usually done such that it simulates the field compaction under the action of a 12.5kg or 22.7kg surcharge mass, depending on the observed consistency level as described in ASTM C1170 / C1170M-08 [7]. In the field, however, the laboratory determined optimum mix can be adequately consolidated using vibratory rollers.

In the literature, a typical MVB time for RCC pavement and overtopping materials ranges between 30 and 40 seconds [8], though RCC with high consistency times, up to 180 seconds, have been successfully compacted in

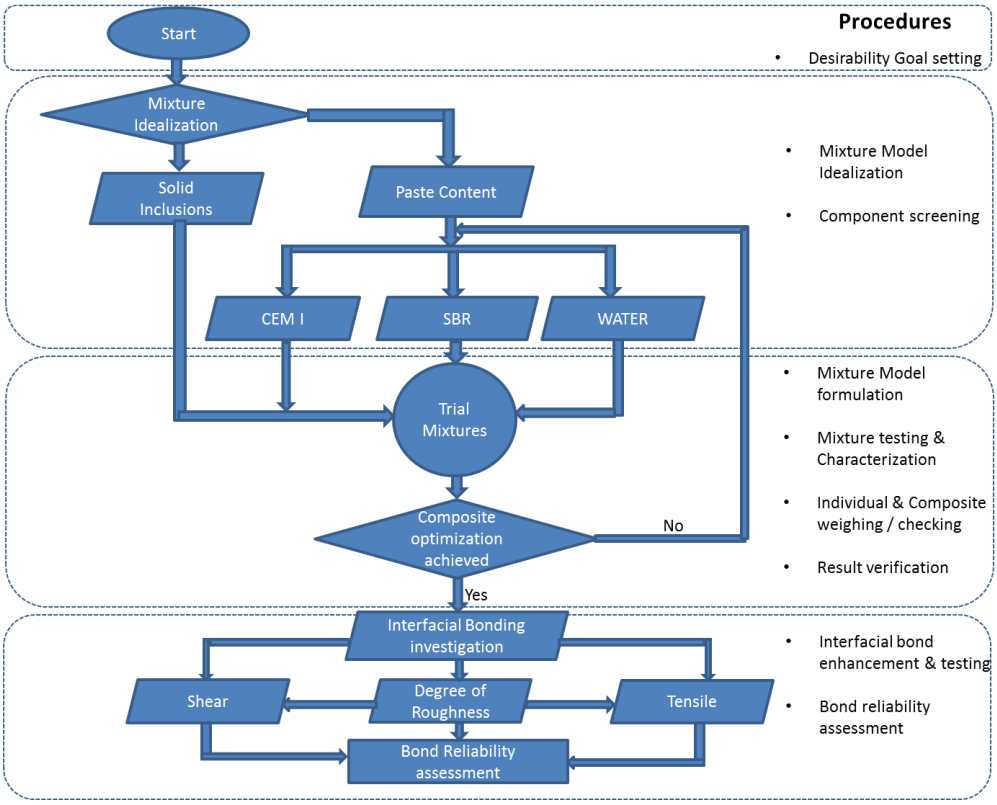

Figure 1: Optimization and methodical procedure flowchart

the laboratory, and could probably be applied in the field when high compaction effort are employed [9]. As a general guide, it is desirable to ensure that the maximum compaction force exerted does not break or crush the aggregates, so as to prevent any change to the granulometric curve. In this respect, an initial MVB time range of 25 to 40 seconds was chosen to define the thresholds of acceptance and rejection, with a target of 35 seconds for the optimum mix.

2.2 Polymer admixture and Steel-fibre additive.

Polymer-modified concretes essentially contain two binder phases made of polymer and cement. Hence their composite behaviour depends on achieving complete cement hydration and polymer film formation processes during the curing period [10-11]. With proper mixture design and curing process, the benefits of Polymer-modified concrete (PMC) over conventional concrete can be enormous, ranging from improved mechanical properties to enhanced bond properties with other materials [12]. In addition, the presence of micro-cracks is also limited in PMC due to its lower shrinkage property. When such cracks develop, they are controlled and bridged to a great extent by the polymer films, thus preventing the likelihood of brittle crack propagation.

For polymer modification of concrete, the use of Styrene-Butadiene Latex / Rubber (SBR) is common, while Polyvinyl Acetate Latex and Poly (vinylidene Chloride (VnC) - vinyl Chloride (VC) latexes are not recommended as cement modifiers [11] due to their respective poor water resistance and chloride ion liberation tendencies. Elsewhere [13], the use of Polyvinyl alcohol (PVA) synthetic polymer which also develops excellent film forming and adhesion has been found useful, its susceptibility to humidity is still an area of concerns to researchers. SBR, though more expensive, generally offers better durability, reduced shrinkage and increased flexibility, as well as being resistant to emulsification in humid conditions.

In ASTM C 150 [14], SBR is recommended for concrete or mortar modification with Type I, II or III Portland cement. Most polymer-modified concretes in the literature are composed of Type I cement and SBR latexes. The use of Type III cement is very limited, except where early rapid strength is required to sustain a service load within 24 hours [15].

The investigation in this work was based on the use of SBR polymer emulsion and CEM I Portland cement due to high early strength requirement. CEM I, according to the new European standard for cement [16], is most suitable for public works where higher early strengths are desirable. Besides, it is compatible with most cement admixtures and additives when used in accordance with manufacturer's recommendations. The specifications and properties of the materials used are given in Table 1, while the combined aggregate grading data is shown in Table 2.

Table 1: Material specifications and physical properties

Materials	Specification and Physical Properties
Cement (CEM I)	CEM I, 52.5N; specific density 3150 kg/m^3
SBR	White emulsion, solid content 46%, water content 54%; specific density 1040 kg/m^3
Coarse aggregate (CA)	Crushed gritstone; size 4.75 -10mm, water absorption 0.5%, particle density on saturated surface-dried 2770 kg/m^3
Fine aggregates (FA)	Quartz river sand, particle density 2670 kg/m^3
Steel Fibre (SF)	Length 35mm, hooked-end, aspect ratio 60

Table 2 Combined aggregate grading

Sieve size	14mm	10 mm	4.75 mm	2.36 mm	1.18 mm	600 µm	300 µm	150 µm	75 µm
Cumulative % passing	100	96	41.2	35.3	33.0	26.8	4.44	1.19	0.14

3.0 Mixture Model, Design and Optimization

The BRCFRPMC used in this study contains six components: Portland cement (CEM I), water, polymer (SBR), fine aggregate (FA), coarse aggregate (CA), and steel-fibre (SF). Its overall composite response, like any concrete mixture, depends essentially on the proportions of its constituents. In practice, several experimental design proportioning methods exist, including Factorial, Response surface, Taguchi, and Mixture design [4]. The choice of a particular design method depends on the approach and the objectives of the experimenter.

For instance, if the experimenter is interested in studying the effects of the amount of each constituent on the response(s), using a factorial design may be appropriate. In this study, Mixture Design method was chosen because its design response depends exclusively on the relative proportions of the input components, and typically its experimental region of interest is more naturally defined [4, 17]. In essence, the design space in Mixture Experiment represents the possible combinations of the relative proportion of each component in the total volume, and usually adds up to 1.

3.1. Mixture Experimental Model

Consider a mixture made of N components such that the i^{th} component occupies x_i of the total space. If the setting for each component space (x_i) is constrained by:

$$x_i \geq 0, \qquad \forall i: \ i \in N$$

and $$\sum_i^N x_i = x_1 + x_2 + x_3 + \cdots + x_N = 1 \qquad (1)$$

then, for a standard mixture experiment, the design region can be represented by a simplex of N vertices with regular sides of $(N-1)$ dimension. Thus, for a blend containing three components as the one illustrated in Figure 2, the design space is an equilateral figure constrained by the conditions stated in equation (1) and its vertices correspond to (1,0,0), (0,1,0), and (0,0,1).

As seen in Figure 2, each vertex represents a pure component where other components are absent; while the centroid depicts a mixture where the three components are present in equal proportion of $(1/3,\ 1/3, 1/3)$; hence, the term simplex-centroid. Numerically, the axis of each component stretches from its vertex ($x_i = 1$) to the midpoint of the opposite side where $x_i = 0$.

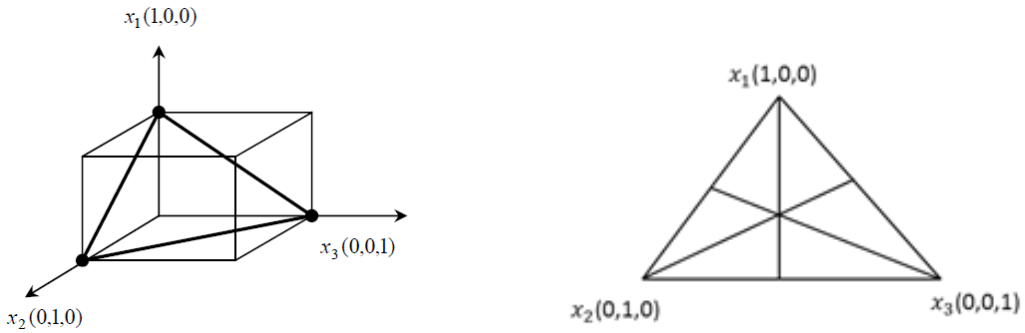

Figure 2: Mixture Design Space for Three components

For modelling purposes, all desired properties can be measured experimentally for each possible mix in the design space and subsequently modelled as a function of the input variables. In many instances, mathematical formulations based on polynomial functions are used, though other forms can be employed [10, 17].

Typically, for a three-component mixture experiment, the usual first order polynomial is given by:

$$E(y) = \beta^* + \sum_i^N \beta_i x_i \qquad (2)$$

Where, β^* is the constant and β_i is the coefficient associated with the model.

Based on the constraint given in equation (1), where $\sum_i^N x_i = 1$; the solution to β_i cannot be uniquely determined. Hence, using the approach suggested by Scheffe [18]; if β^* is multiplied by $\sum_i^N x_i = 1$, then equation (2) becomes:

$$E(y) = \sum_i^N (\beta^* + \beta_i) x_i \qquad (3)$$

Typically equation (3) is re-parameterized in the form:

$$E(y) = \sum_{i=1}^N \beta_i x_i \qquad (4)$$

So that its quadratic polynomial can be written as:

$$E(y) = \sum_{i=1}^N \beta_i x_i + \sum \sum_{i<j}^N \beta_{ij} x_i\, x_j \qquad (5)$$

Where, β_{ij} represents the nonlinear or quadratic blending term. When β_{ij} is positive, the term is synergistic, while a negative value suggests an antagonistic blend response.

In addition, where full cubic and special cubic functions are considered, equations (6) and (7) result respectively:

$$E(y) = \sum_{i=1}^N \beta_i x_i + \sum \sum_{i<j}^N \beta_{ij} x_i\, x_j + \sum \sum_{i<j}^N \delta_{ij} x_i\, x_j (x_i - x_j) + \sum \sum_{i<j<k} \sum \beta_{ij} x_i x_j x_k \qquad (6)$$

$$E(y) = \sum_{i=1}^N \beta_i x_i + \sum \sum_{i<j}^N \beta_{ij} x_i\, x_j + \sum \sum_{i<j<k} \sum \beta_{ij} x_i x_j x_k \qquad (7)$$

Accordingly, the appropriate model for an experiment usually follows the method of analysis of variance (ANOVA).

3.2. Mixture Experiment Optimization Techniques

Following the three-component design space shown in Figure 2, it is evident that no viable concrete mixture can be obtained over the entire simplex-space without constraining the mixture design to a sub-region of the equilateral triangle. The constraint is usually obtained by applying a lower bound, or an upper bound, or both restrictions on the mixture components in addition to the initial condition that the total of all component proportions must add up to 1. In this respect we write that:

$$\left.\begin{array}{ll} 0 \le L_i \le x_i & for\ lower\ limit \\ 0 \le x_i \le U_i & for\ upper\ limit \\ 0 \le L_i \le x_i \le U_i \le 1 & for\ combined\ limits \end{array}\right\} \qquad (8)$$

$where, i = 1,2, \ldots, N;\ \ L_i = Lower\ limit;$
$U = U\ pper\ limit; and\ x_i = component\ proportion$

By definition, when a mixture is constrained by the restrictions given in inequalities (8), it is referred to as Constrained Mixture Design. In the present study, a classical constrained fitting model based on Extreme-Vertices Design (EVD) approach of [19] was adopted.

In the model, both lower and upper bounds were set a priori, and a list of all combinations based on $[N(2)^{N-1} + 1]$ possible blends was made. In addition to the choice of model, an overall desirability function (D) was incorporated and used as a metric for multi-criteria optimization.

For each criterion, two values, 0 and 1, were defined, such that the desirability scale satisfies the condition

$0 \leq d(y_i) \leq 1$. In this case, '0' indicates that one or more criteria lie outside their acceptable values, while '1' corresponds to the ideal response. The conditions for acceptance or rejection generally depend on the set goal, i.e. the direction of optimization – maximum, minimum or target; in reference to equation (9), (10), or (11):

Here, a maximized response indicates that a larger value is better, and its desirability is calculated by:

$$d(y_i) = \begin{cases} 0 & y_i < L \\ \left(\frac{y-L}{T-L}\right)^{r_i} & L \leq y_i \leq T \\ 1 & y_i > T \end{cases} \quad (9)$$

while, a minimized response shows that a smaller value is better, with its desirability given by:

$$d(y_i) = \begin{cases} 1 & y_i < T \\ \left(\frac{U-y_i}{U-T}\right)^{r_i} & T \leq y_i \leq U \\ 0 & y_i > U \end{cases} \quad (10)$$

Finally, the "target" indicates the best response, and its desirability corresponds to:

$$d(y_i) = \begin{cases} 0 & y_i < L \\ 0 & y_i > U \\ \left(\frac{U-y_i}{U-T}\right)^{r_i} & T \leq y_i \leq U \\ \left(\frac{y_i-L}{T-L}\right)^{r_i} & L \leq y_i \leq T \end{cases} \quad (11)$$

Where y_i is predicted value of ith response; T is target value; U is highest acceptable value; L is lowest acceptable value; and r_i is weight of ith desirability function. Based on the conditions given in equations 9, 10 and 11, a multi-response numerical optimization was performed, during which the optimum mix maximizes the weighted geometric mean of individual desirability function ($d(y_i)$) over the feasible composite space. In the process, a model with equal weight was adopted; hence, the composite desirability takes the form:

$$D = [d(y_1) \times d(y_2) \times \ldots \times d(y_n)]^{1/n} \quad (12)$$

Where, n is total number of all individual responses.

3.3. Optimum Mixture Design Method

Hypothetically, BRCFRPMC can be considered as a matrix of two phases: the paste (P) phase and the solid inclusion (SI) phase. The paste phase consists of WATER and Portland cement (CEM 1) modified with SBR, and occupies about 39% by volume of the total mixture; while the remaining 61% is filled with solid inclusion phase comprising CA, FA and SF.

By this hypothesis, the paste phase was considered central to consistency and optimum bond requirements, in order to ensure ease of applicability during vibrating compaction and satisfactory composite behaviour of the overlay system. Therefore, the mixture experiments here investigate variable combinations of the paste constituents that will be required for optimal performance when mixed with a constant proportion of the solid inclusions. Table 3 represents the proportion of the mixture components.

It should be noted that the total volume shown in Table 3 indicates a theoretical air-free mixture, while the variable proportions of SBR and WATER depend on the amount of CEM I.

Tables 3: Mixture proportion of solid inclusions phase and paste phase

	Solid Inclusion phase			Paste phase		
Material	CA	FA	SF	CEM I	SBR	WATER
Weight (kg)	952.5	635	117	≤ 635	Variable	Variable
Volume (m^3)	0.35	0.24	0.015	-	-	-
Total Vol. (m^3)	0.61			0.39		

In this experiment, the maximum cement content was restricted to ≤635kg, while the trial range of variabilities for Water-Cement (W/C) and Polymer-Cement ratio (P/C) was constrained between 18% - 22% and 10% - 15% respectively.

It has been shown that (P/C) ratios ≥ 20% impair both compressive strength and elastic modulus properties considerably [20], while ratios ≤ 5% are insufficient to create any additional continuous phase within the hardened concrete matrix. In addition, the choice of high cement contents was based on ACI guidelines [21-22]. Cement contents in the range of 600 – 700 kg/m^3 are typically recommended for bridge deck and pavement overlays modified with SBR, for enhanced bonding and strength development.

Although, the use of high cement contents to enhance bonding and strength could also results in high risk of shrinkage and thermal cracking; with adequate polymer content and sufficient inclusion of steel-fibre, usually within 1.5% - 2.0% by volume of the mix [23], the risks can be minimized. Thus, in the present work, a fixed volume of 1.5% steel-fibre was added in the mix at a maximum aspect ratio of 60, thereby limiting the likely effects of curling [24]. In addition, the use of fibre reinforcement helps curtail possible reflective cracking associated with most bonded overlay systems. Fibre reinforcement generally enhances both tensile strength and toughness of cementitious materials.

From above, since the amount of solid inclusions (SI) shown in Table 3 is held fixed for all possible mix combinations of the paste (P), it follows that the proportion of (SI) to (P) can be implemented as a three-component mixture experiment, involving only SBR, CEM 1, and WATER. Thus, in Table 4, if the upper and lower bounds are applied on $[SBR/CEM1]$ and $[WATER/CEM1]$ based on the variability limits discussed above, then the actual amount of each component can be estimated. Table 5 presents the proportion of each component as a fraction of a constant total paste.

In Table 5, based on the conditions stated in equation (1), the sum of each possible paste combination (each row) is constrained to a total of 1. From the resulting lower and upper bound values, an Extreme Vertices Design (EVD) was implemented to formulate some possible mix combinations based on the following constraints:

$$0.078 \leq x_1 \leq 0.117$$
$$0.141 \leq x_2 \leq 0.172$$
$$0.711 \leq x_3 \leq 0.781$$

Table 4: Actual range of Cement Contents

$Range\ Limit$	$\left(\frac{SBR}{Cem}\right)$ (%)	$\left(\frac{Water}{Cem}\right)$ (%)	SBR (kg)	$Water$ (kg)	$Cem.\ (kg)$	$Total\ amount\ (kg)$
Lower	10	18	63.5	114.3	635	812.8
Upper	15	22	95.25	139.7	577.85	812.8

Table 5: Paste Components Proportion

$Range\ Limit$	$SBR\ (x_1)$	$WATER(x_2)$	$CEMENT\ (x_3)$	$TOTAL$
Lower	0.078	0.141	0.781	1.0
Upper	0.117	0.172	0.711	1.0

The implementation of the mixture model was done on the initial assumption that a second-degree (quadratic) design will be sufficient. In the design, 4 vertex design points were created with 4 augmented axial points. In addition, in order to ensure a more robust model, 4 interior and 1 centre points were incorporated. In total, these make up 13 points on which all required properties were associated.

The corresponding coordinates and design output space are depicted in Table 6 and Figure 3 respectively. In Figure 3, the thick dashed line defines the design region, while the dots represent the design points. From Table 6, the basis for batching by weight in kg of each paste constituent was established. Further, in order to allow for sufficient repeatability, a total of five runs for each design point were implemented per specified response. Subsequently, ANOVA was performed with Minitab statistical software [25]. In the analyses, components and models with p-value ≤ 0.05 were selected as viable. Also, for each chosen model, checks on normality, outliers, and consistency of the residuals were carried out accordingly.

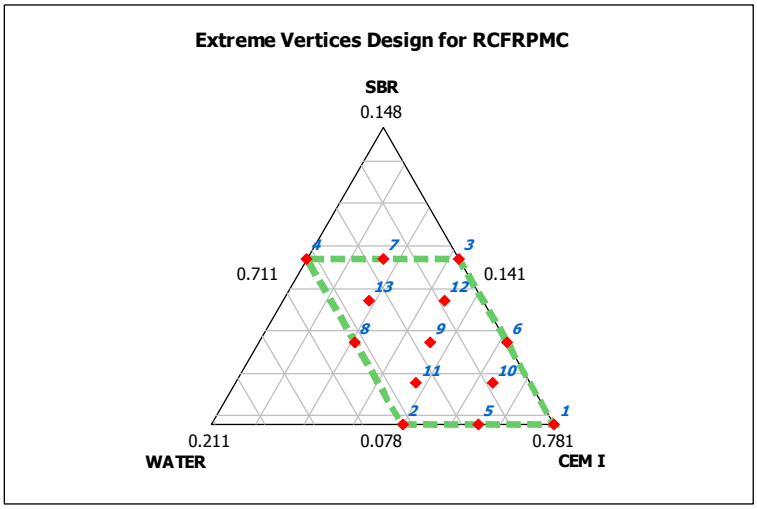

Figure 3: Extreme Vertices Design for BRCFRPMC

Table 6: BRCFRPMC Paste Component Proportions

Design point	*Pt Type*	*SBR* (x_1)	*WATER* (x_2)	*CEM I* (x_3)
1	1	0.078	0.141	0.781
2	1	0.078	0.172	0.750
3	1	0.117	0.141	0.742
4	1	0.117	0.172	0.711
5	2	0.078	0.157	0.766
6	2	0.098	0.141	0.762
7	2	0.117	0.157	0.727
8	2	0.098	0.172	0.731
9	0	0.098	0.157	0.746
10	-1	0.088	0.149	0.764
11	-1	0.088	0.164	0.748
12	-1	0.107	0.149	0.744
13	-1	0.107	0.164	0.729

Table 7: BRCFRPMC Components Proportion

Design point	*Mix ID*	*Components Quantity (kg)*					
		SBR	*WATER*	*CEM I*	*CA*	*FA*	*SF*
1	M1	63.40	114.60	634.80	952.50	635.00	117.00
2	M3	63.40	139.80	609.60	952.50	635.00	117.00
3	M7	95.10	114.60	603.10	952.50	635.00	117.00
4	M9	95.10	139.80	577.90	952.50	635.00	117.00
5	M2	63.40	127.20	622.20	952.50	635.00	117.00
6	M4	79.25	114.60	618.95	952.50	635.00	117.00
7	M8	95.10	127.20	590.50	952.50	635.00	117.00
8	M6	79.25	139.80	593.75	952.50	635.00	117.00
9	M5	79.25	127.20	606.35	952.50	635.00	117.00
10	M12	71.32	120.90	620.57	952.50	635.00	117.00
11	M10	71.32	133.50	607.97	952.50	635.00	117.00
12	M11	87.17	120.90	604.72	952.50	635.00	117.00
13	M13	87.17	133.50	592.12	952.50	635.00	117.00

Note: The specified water proportion includes the free water in the aggregates, the water in the latex, and the added water. The Mix ID was discretionarily chosen, and represents the batching order.

Figure 4: Representative mixtures: (a) M1 in the Vebe cylinder (b) 22.7 kg surcharg mass mounted on test specimen (c) Fully consolidate test specimen with a ring of mortar around the disk (d, e, f) Top finished surface of Mix 1, Mix 2 and Mix 3 after consolidation

4.0 Experimental Description, Results and Analysis

4.1 MVB and Wet Density tests

In order to determine the suitability range of the mixture proportions listed Tables 7, the test procedures of MVB and wet density used complied with ASTM C1170 / C1170M-08 [7], while the general mixing procedure for each batch followed ASTM C1439-99 [26].

On the basis of visual observations of some trial test specimens, procedure requiring 22.7kg surcharge mass was deemed fit and subsequently maintained all through the experiments. Clearly, the use of a single surcharge mass for all test specimens helps comparison in results. Figure 4 shows the visual appearance of some representative mixtures consolidated under the action of the surcharge mass.

The overlaid contour result shown in Figure 5 depicts the feasible space, and indicates that only few samples experienced full consolidation within the desirable consistency-time range of 25 and 40 seconds. The corresponding wet density response for each test mixture is shown in Table 8.

Usually, for most RCC mixtures, it is expected that the apparent maximum density (AMD) after rolling vibration shall be $\geq 98\%$ of the theoretical air-free density (TAFD), but where no AMD is specified a priori, compaction shall achieve density $\geq 96\%$ TAFD [27]. Hence, in order to simulate these compaction levels, cylindrical specimens were cast from each possible mixture and compacted with a modified electric plate compactor for 20 seconds each layer of four per specimen. Each specimen measured 200mm high by 100mm diameter, and density measured in accordance to ASTM D792 [28]. Note, by using similar range of AMD values as those specified here, it's possible to assess the consolidation level of each mixture for equal period of vibration or compaction.

The TAFD and air-content (%) shown in Table 8 were determined using the procedures given in ASTM C138 [29] and ACI 211.3 [30]. The result in Table 8 demonstrates that for similar condition of compaction, different levels of consolidation were achieved. The optimum mixture based on the two properties defined here, attaine about 98.4% TAFD, which in this case has a consistency-time of 32 seconds when vibrated on the MVB table. As seen, the consistency times due to MVB test fall generally between 20 and 80 seconds with a statistical mean of 34.1 seconds. The overall compacted density as seen falls within the limit $97.1 \pm 1.34\ \%TAFD$. Though, this limit falls slightly below the

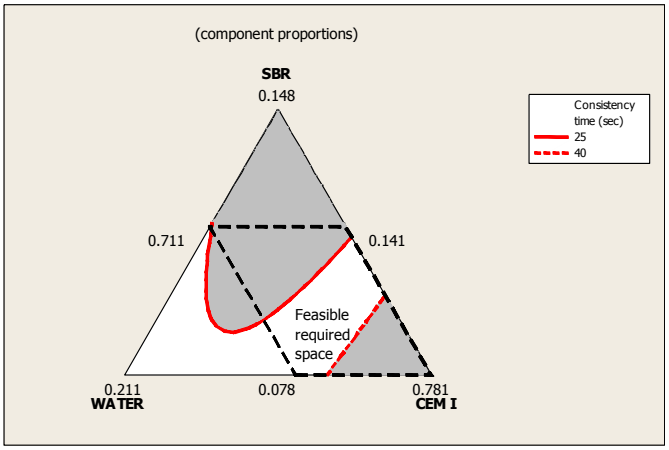

Figure 5: Contour Plot of Consistency-time (sec)

Table 8: Consistency and Density properties of test specimens

Property Measured	*Test specimen mixture ID*												
	M1	*M2*	*M3*	*M4*	*M5*	*M6*	*M7*	*M8*	*M9*	*M10*	*M11*	*M12*	*M13*
Consistency time (sec.)	78	50	32	40	34	29	24.5	22.8	20.7	30.1	23	37	22
Wet density (kg/m3)	2334	2425	2476	2418	2418	2367	2442	2424	2402	2429	2447	2382	2442
Compacted density (%TAFD)	95.8	97.2	98.4	96.9	97	96.1	98	97.4	96.7	97.7	98.3	96.7	98.0
Air-Content (%)	4.24	2.81	1.57	3.13	3.01	3.88	2.04	2.61	3.32	2.29	1.74	3.29	2.00

desirable AMD value ($\geq 98\%\, TAFD$) for most of the test mixtures, three mixtures – M3, M11, and M13 – exhibit considerable high response in the vicinity $\geq 98\%\, TAFD$, while all other mixtures, except M1, show values $\geq 96\%$. At this stage, only M3 seems to satisfy both consistency and density criteria.

Further, each of the three responses in the on-going analysis was analysed by fitting and verifying each model. In all cases, model selection allows prediction based on a quadratic relation, but through the analysis of variance (ANOVA), a linear model may provide a sufficient fit to the data. The ANOVA table for consistency-time, wet density, and compacted density is shown in Table 9.

In Table 9, the rows with "linear" are used to test whether the coefficients of linear terms are equal, while the rows with "quadratic" examine whether any quadratic term is a non-zero coefficient. As seen in Table 9, it is clear that the p-values associated with both linear and quadratic models in each response are less than 0.05. Hence, it was assumed that either a linear or a quadratic model is significant at an $\alpha -$ level of 0.05, thus will suffice to fit the models. In this regard, quadratic models were adopted. The resulting model for each response is presented in Table 10. For the avoidance of repetition, it should be mentioned that the analyses for other responses examined in this study followed a similar way.

Table 9: ANOVA table for consistency-time, wet density and compacted density

Analysis of Variance for Consistency time (sec) (Paste component proportions)

Source	DF	Seq SS	Adj SS	Adj MS	F	P
Regression	5	13656.7	13656.7	2731.4	155.4	0.000
Linear	2	10579.9	277.4	138.7	7.9	0.001
Quadratic	3	3076.8	3076.8	1025.6	58.4	0.000

Analysis of Variance for Wet Density (kg/m3) (component proportions)

Source	DF	Seq SS	Adj SS	Adj MS	F	P
Regression	5	57988.2	57988.2	11597.6	26.9	0.000
Linear	2	7789.7	6908.9	3454.4	8.0	0.001
Quadratic	3	50198.5	50198.5	16732.8	38.7	0.000

Analysis of Variance for % Compacted density (Paste component proportions)

Source	DF	Seq SS	Adj SS	Adj MS	F	P
Regression	5	39.0	39.0	7.8	25.8	0.000
Linear	2	3.2	6.2	3.1	10.3	0.000
Quadratic	3	35.9	35.9	11.9	39.5	0.000

Table 10: Quadratic models for Consistency-time, Wet density, and Compacted density

Property	Model Equation	S.D	R-sq.
Consistency-time(sec)	$8346(x_1) + 9676(x_2) + 1307(x_3) - 168(x_1x_2) - 16291(x_1x_3) - 17876(x_2x_3)$	4.2	92.9
Wet density (kg/m^3)	$44050(x_1) - 4404(x_2) - 1857(x_3) - 94906(x_1x_2) - 26791(x_1x_3) + 83897(x_2x_3)$	20.8	70.0
Compacted density(%TAFD)	$1547(x_1) - 619(x_2) + 5(x_3) - 3701(x_1x_2) - 1112(x_1x_3) - 1517(x_2x_3)$	0.6	70.0

Where: S.D= standard deviation; $x_1 = SBR$; $x_2 = WATER$; and $x_3 = CEM1$

4.2. Elastic Modulus and Compressive Strength tests.

The test specimens used for both compressive and elastic modulus responses were cast into cylinder steel mould and compacted with a modified plate vibrator. The compaction effort was maintained for 20 seconds each layer of four per specimen. Each specimen was afterward covered with a light polythene sheet and cured in the mould at 60% RH laboratory condition for 18 hours. After de-moulding, specimens were stored in the curing tank at 100% RH for 24 hours, followed by air curing under laboratory condition. Compressive and elastic modulus tests were performed at 3 and 28 days in accordance to ASTM 469 [31] procedures. Each cylinder measured 200mm high by 100mm diameter. For both experimental tests, five replicates were implemented each for all possible mixtures shown in Table 7.

The compressive and elastic modulus responses are shown in Figure 6. Here, the material performance of the optimum overlay mixture was assessed in terms of its structural response and elastic compatibility with the substrate material. Table 11 represents the mixture constituents of the substrate material used in this work. The substrate material was made of a typical high strength ordinary Portland cement concrete (OPCC). The OPCC was cured for 28 days in water and subsequently in air till when tested at 90 days. It exhibits a characteristic compressive strength of 47MPa, and a mean tensile strength and elastic modulus of 3.97MPa and 22.3GPa respectively.

As seen in the contour plots shown Figure 6 (a & b), strength decreases clearly with increase in WATER and SBR proportions, but increases as the proportions of CEM I increase; while the contours due to elastic modulus in Figure 6 (c & d) show that SBR has a clear reducing effect on the overall elastic response. The observed mean compressive strengths within the design space at 3 and 28 days mostly fall above 32MPa and 50MPa, while the corresponding elastic moduli range between 11.5 – 17.5GPa and 17 – 26GPa respectively. Following similar analysis as in Table 9, the resulting regression models for compressive strengths and Elastic Moduli responses for ages 3 and 28 were determined and presented in Table 12.

Table 11: OPCC material constituents

Material	*CEM I*	*CA*	*FA*	*WATER*	*TOTAL*
Quantity (kg/m^3)	400	1116	684	200	2400
Specific / particle density (kg/m^3)	3150	2770	2670	1000	-

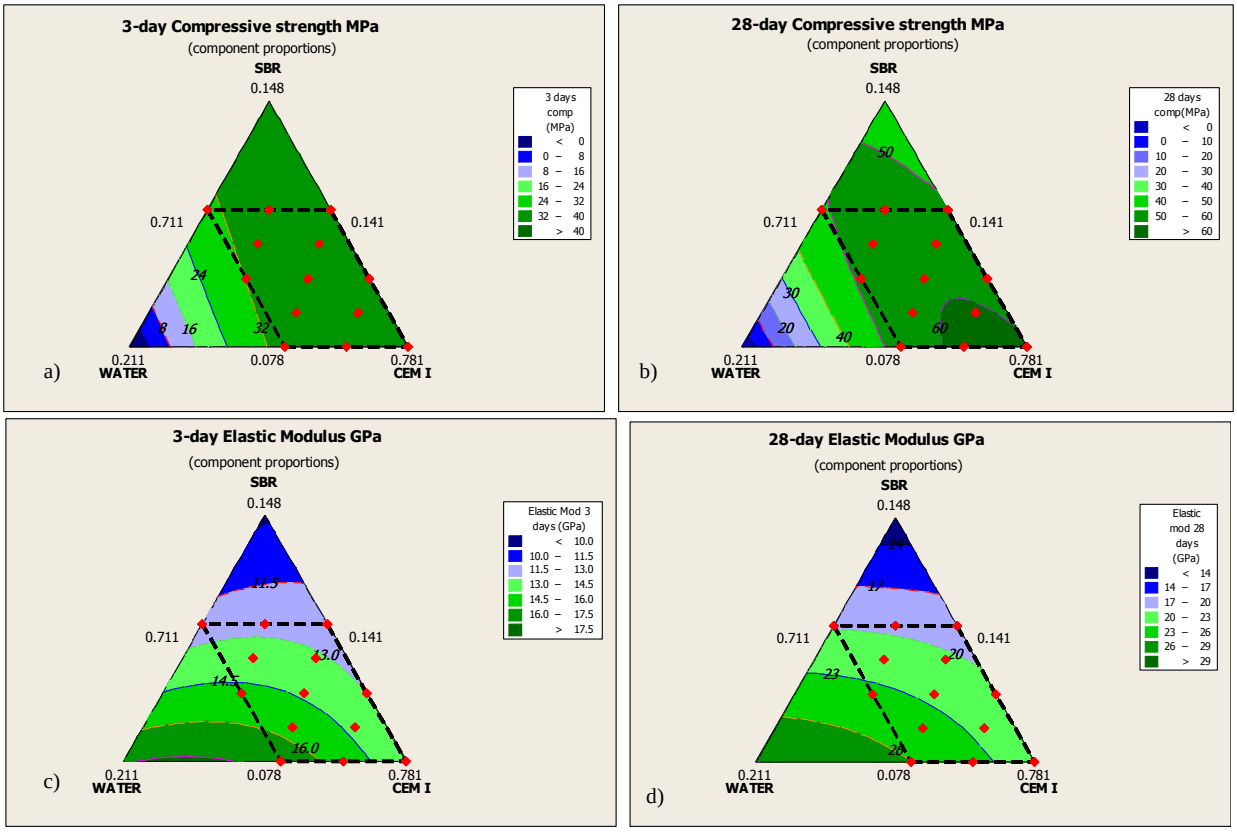

Figure 6: Mean Compressive strengths and Elastic Moduli responses at 3 and 28 days

Table 12: Quadratic models for Compressive strengths and Elastic Moduli

Property	*Model Equation*	*S.D*	$R-sq$
Compr. strength (MPa) 3-day	$251(x_1) - 9665(x_2) - 260(x_3) + 12625(x_1x_2) - 740(x_1x_3) + 13538(x_2x_3)$	1.9	70.0
Compr. strength (MPa) 28-day	$-1652(x_1) - 13412(x_2) - 286(x_3) + 23080(x_1x_2) + 656(x_1x_3) + 18262(x_2x_3)$	1.8	83.2
Elastic Moduli (GPa) 3-day	$-305.3(x_1) - 763.9(x_2) - 79.2(x_3) - 745.1(x_1x_2) + 784.7(x_1x_3) + 1516.1(x_2x_3)$	0.07	99.8
Elastic Moduli (GPa) 28-day	$-1358251(x_1) - 478(x_2) - 76(x_3) + 165(x_1x_2) + 2041(x_1x_3) - 1160(x_2x_3)$	0.1	99.8

Where: S.D=standard deviation; $x_1 = SBR; x_2 = WATE;$ and $x_3 = CEM1$

From the analyses, the optimum overlay mixture was selected based on the desirability requirements specified in some selected codes of practice and published technical papers. In the US, for instance, due to severe exposure condition of concrete pavement and bridges, the minimum compressive characteristic strength for most overlays is usually limited to around 25 - 30MPa [32]. Similarly, EC2 [33] specifies a minimum compressive strength of C30/37*. Consequently, a minimum target characteristic cylinder strength of 30MPa was set for the overlay within the first 72 hours of placing. In the long-term (say 28 days and over), however, the overlay material should have equal or greater strength than the substrate [34]. Also, in terms of elastic property compatibility requirements, the elastic modulus is required to be similar to that of the substrate [34].

From the target characteristic strength set above, the corresponding target mean strength was estimated based on the computed minimum and maximum standard deviation values associated with the results. At 5% defect, for age 3, the limits of the target mean strength fall within $32.7 \pm 1.7MPa$; while for age 28, we

employed OPCC characteristic compressive strength as our target. Thus, for age 28, the estimated limits of the target mean strength fall within $50.3 \pm 1.9MPa$. Hence, by comparing these limits with the response contours shown in Figure 6 (a & b), it shows that all mixtures used in this experiment satisfied the strength requirements for both early age of 3 days and matured age of 28 days.

Similarly, for elastic properties compatibility, we constrained the choice of optimum response within 5% tolerance of that of the substrate OPCC; thus, the optimum limits fall between 21.2GPa and 23.4GPa. From here, by comparing these limits with the response contours shown in Figure 6 (c & d), it is evident that at age 3, none of the mixtures employed in the experiment satisfied the elastic compatibility requirement; hence, the resulting desirability automatically yields zero.

Note that the observation here is commonplace with newly cast fresh cementitious materials, and thus indicates that the material design of cementitious overlays typically introduces some degree of intrinsic elastic mismatch problem at early age. Intuitively, a rational solution at this stage of the analysis is to allow for some level of "trade-off" between what is intrinsic and what to design against.

Clearly, a direct enhanced mixture solution may not always be economical or practicable due to its autogenous nature, but its consequential effects on the composite elements can be minimized, especially at the interface, by ensuring that adequate bonding between the overlay and the substrate is achieved. In this respect, our overall composite desirability level was determined using the 28-day elastic modulus response.

4.3 Composite Desirability analysis and results

In Table 13, the desirability limits for each response (property) set above are summarized, while Figure 7 illustrates the optimal composite desirability result.

Table 13: Summary of multi-response desirability limits

Property	*Goal*	*Lower*	*Target*	*Upper*	*Weight*
Consistency-time (sec)	Target	25.0	35.0	40.0	1
Compacted density (%TAFD)	Maximize	96.0	98.0	-	1
Compressive strength (MPa) 3-day	Maximize	31.02	34.4	-	1
Compressive strength (MPa) 28-day	Maximize	48.4	52.2	-	1
Elastic Modulus (GPa) 28-day	Target	21.2	22.3	23.4	1

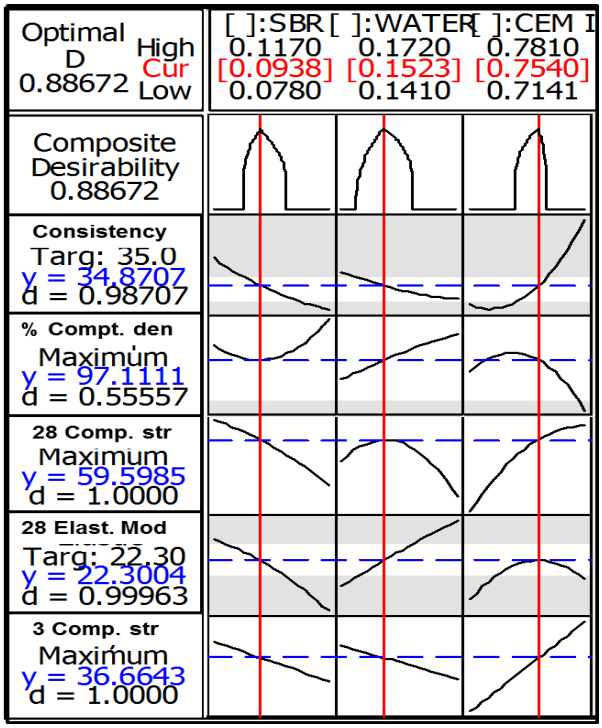

Figure 7: Composite optimization Response plot

Figure 7 depicts the composite desirability response curves implemented with Minitab statistical software [25]. The input variable settings that optimize all responses are given in Table 13. Our choices of goal, lower, target, and upper limits were used to define the desirability function for each individual response as earlier expressed in equations 9 to 11. In addition, equal weight of 1 was assigned to all the responses, therefore permitting composite desirability analysis based on equation 12 to be implemented. In the results shown in Figure 7, the overall desirability yields 0.89, while the desirability value for individual response is denoted by "d". As seen, the composite desirability value and the individual desirability for each predicted property show sufficient closeness to 1 as desired.

As observed in Figure 7, the curves under each column show the property responses as each paste component employed for the computational experiment varies from its upper to its lower bound. Note that the bounds used here are based on the initial prescribed constraints drawn from Table 5. The constraints are done such that when one component increases in the mixture, the other two components decrease accordingly, due to the condition that the overall proportion must add up to 1. From the results, the predicted optimum response "y" associated with each property corresponds strictly to the optimum mixture proportion.

The results indicate that consistency-time decreases when SBR and WATER proportions increase beyond the optimum proportion, but tends to increase with increased CEM I. Similarly, as seen, increase in both SBR and WATER proportions beyond the optimum decreases the compressive strength which agrees with the results shown earlier in Figure 6 (a & b). On the other hand, response due to compacted density shows that density generally decreases with increased CEM I proportion, though increasing the proportions of both SBR and WATER above the optimum may yield a higher response. For elastic modulus, increasing SBR and CEM I proportions above the optimum lowers the response, while increasing WATER may give a higher value.

The optimum mixture proportion as shown in the Figure 7 is indicated by the square brackets at the top of each column. It demonstrates that the optimum predicted responses are recorded when the proportions of SBR, WATER, and CEM I correspond to 0.0938, 0.1523 and 0.7540 respectively in the paste content. Thus, for batching by weight, each optimum component indicated here is multiply by 812.8kg which gives the needed paste weight in the total mix. Table 14 gives the resulting optimum amount by weight for a complete mixture, while Table 15 summarizes its predicted responses based on the results shown in Figure 7, and its actual responses when each property was subsequently tested experimentally for verification with three replicates each.

From Table 15, it is clear to a great extent that the actual response properties of the optimum mixture correlate reasonably well with the predicted and the desirable values. Besides, visual observations indicated that the mixture was neither too dry nor too wet as expected; and no lumping, pumping or sinking was generally observed during compaction. Thus, we proceeded from here to assess the interfacial bond capacity of the optimum mixture with the underlying OPCC substrate by employing methods of direct shear and indirect tensile tests.

4.4 Interfacial Bond tests and results

In practice, where composite sections are required to transmit stresses across an interfacial plane, the bond capacity of the interface is very crucial and must therefore be designed to withstand all shearing and tensile loads [35-36]. The bond capacity as well-known depends on the interlocking action of the aggregates, the cement-to-cement adhesion at the interface, and the dowel action of the rebar where shear reinforcement is present [35, 37]. In the present work, the use of shear connectors was not considered; the interlocking action of the interface was enhanced through surface roughening of the substrate, while the adhesion at the interface relies on the chemical grip of the optimum paste mixture described in Table 14.

Table 14: Optimum BRCFRPMC material constituents

Material	*CEM I*	*WATER*	*SBR*	*CA*	*FA*	*SF*	*TOTAL*
Quantity (kg/m^3)	612.9	123.8	76.2	952.5	635.0	117.0	2517.4
Specific / particle density (kg/m^3)	3150	1000	1040	2770	2670	7800	-
Volume in mixture (m^3)	0.195	0.124	0.073	0.34	0.24	0.015	0.987

Note: Air Content = 100 (1- V_t) = 100 (1-0.987) = 1.3%

Table 15: Response properties of Optimum mixture

Property	*Predicted Response Value*		*Actual (Measured) Response Value*		*Desirable Value / range*	
	Age-3	*Age-28*	*Age-3*	*Age-28*	*Age-3*	*Age-28*
Consistency-time (sec.)	34.9		34.1		35.0	
Compacted Density (%TAFD)	97.11		98.03		$96 \leq TAFD \geq 98$	
Air-Content (%)	2.89		1.97		1.30	
Compressive strength MPa)	36.7	59.6	35.2	54.9	$\geq 32.7 \pm 1.7$	$\geq 50.3 \pm 1.9$
Elastic Modulus (GPa)	14.3*	22.3	12.9	20.0	22.3	

*Note: *Predicted Elastic Modulus at age 3 computed from Table 12.*

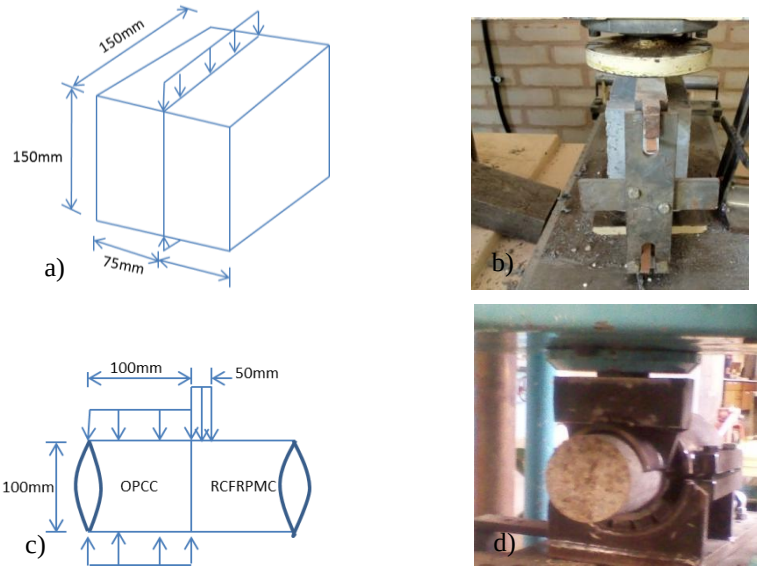

Figure 8: (a-b) Tensile splitting test (c-d) Direct cylinder (Guillotine) shear test

In the experiments, seven replicates were implemented each for interfacial tensile and shear strength tests. The interfacial splitting tensile strength test adhered to the provisions given in BS EN 12390-6:2000 and ASTM C496 [38-39], while the direct shear test complied with Iowa Testing Method 406-C [40]. The test specimens were made of bonded overlay materials on substrate concrete (OPCC-BRCFRPMC composites). The tensile tests employed 150 x 150 x 75mm identical bonded prismatic square sections, while the shear tests were made of identical bonded 100 x 100mm diameter cylinder sections, and the loadings applied as shown in Figures 8. Here, the use of cylinder specimens simulates conventional method where core samples are taken from site for testing in the laboratory.

The procedures for casting and preparing the substrate OPCC surface were similar in both experiments. In both tests, the hardened OPCC specimens were classified into three distinct surface textures. The classifications follow different degree of roughness intentionally induced on some specimens, while others were left un-roughened as shown in Figure 9. In Figure 9, the OPCC interface characterization defined as smooth corresponds to the interface cast directly against the mould with no further treatment added. These specimens were assigned 0.0mm (baseline texture). The other two classifications were roughened intentionally, prepared by rubber brushing at two different controlled levels, just about four and half hours after casting.

Note, the reason for preparing the surface just after the initial setting period of the OPCC was to ensure texture repeatability for specimens required for similar degree of roughness during the experiments. It was observed that once the mortar in the concrete matrix becomes hardened, the process of exposing the aggregates or achieving similar degree of texture for effective interlocking action becomes problematic, as it tends to leave some loosed fractured surface behind. Such cracks often can serve as points of weak bond at the plane of the interface.

Hence, for laboratory investigation purposes, the adopted method affords a better surface preparation compared to gunning, drilling or any forceful blasting attempted initially. In the field however, the use of high-pressure water jetting can be employed.

Figure 9: Interface texture (a) smooth interface (b) Roughened interface (15-stroke each lateral direction) (c) Roughened interface (30-stroke each lateral direction interface)

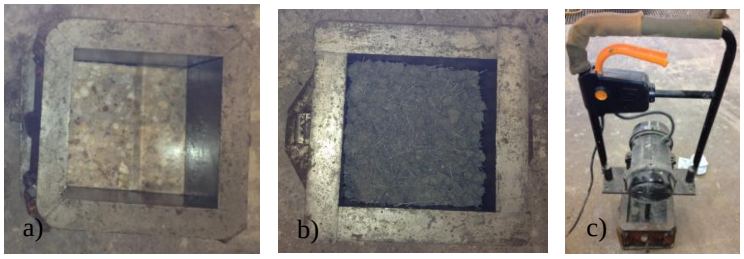

Figure 10: Bonding of fresh overlay on old (hardened) concrete: a) Mould containing old OPC, b) Overlay material placed over old OPC prior to compaction, c) Modified electric plate compactor applied at 20sec. per layer

The texture figures shown in Figure 9 are the mean values obtained by sand-patch measurement method [41-42]. Before placing the sand; it was ensured that the surface was dry and non-sticky. In this respect, all specimens measured were taken out of the curing tank and allowed to dry in the laboratory atmospheric condition for about five days before placing the sand.

In general, curing period of 90 days in water tank was allowed for all substrate specimens, after which they were removed and cured in air for 5 days. The interface was kept clean, free of grease smear, sprayed with tap water and allowed to dry so that no free water was left on the surface prior to placing and compacting the fresh overlay material with the modified plate vibrator shown in Figure 10. The compaction effort was maintained for 20 seconds each layer of three per specimen.

Each specimen was afterward covered with a light polythene sheet and cured in the mould at 60% RH for about 18 hours. After de-moulding, specimens were stored in the curing tank at 100% RH for 24 hours, followed by air curing under laboratory condition. In both experiments, tests were conducted at 3, 14 and 28 days.

The composite splitting test specimens were loaded continuously in compression between two steel platens to failure along two axial lines which are diametrically opposite. As in the codes [38-39], standard compression-testing machine was used, with loading rates ranging between 0.01 and 0.04 MPa/s for different age tests. The load was applied through 10mm wide by 4mm thick hardboard strips to prevent local damage.

The resulting splitting tensile strength computed from equation 13 [43] are presented in Figure 12. For the shear tests, the laboratory fabricated set-up loaded in compression is illustrated in Figure 8(d). The loading rates in this case also vary for different age test, but generally within 0.01 and 0.02MPa/sec. The shear bond strength was determined based on equation 14, by dividing the failure load by the interface cross sectional area.

In addition, after testing each shear specimen to failure as shown in Figure 11, splitting test was conducted on the remaining half cylinder portion of the overlay and its tensile strength was evaluated using equation 15 [44]. It should be noted that only four half cylinder specimens were tested in splitting, the remaining three

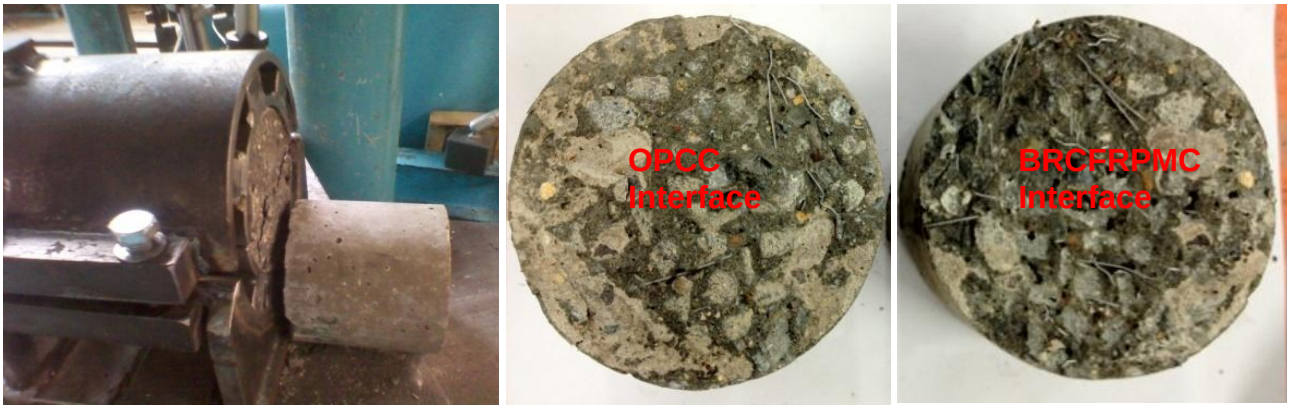

Figure 11: OPCC-BRCFRPMC Bi-interface after tested to failure

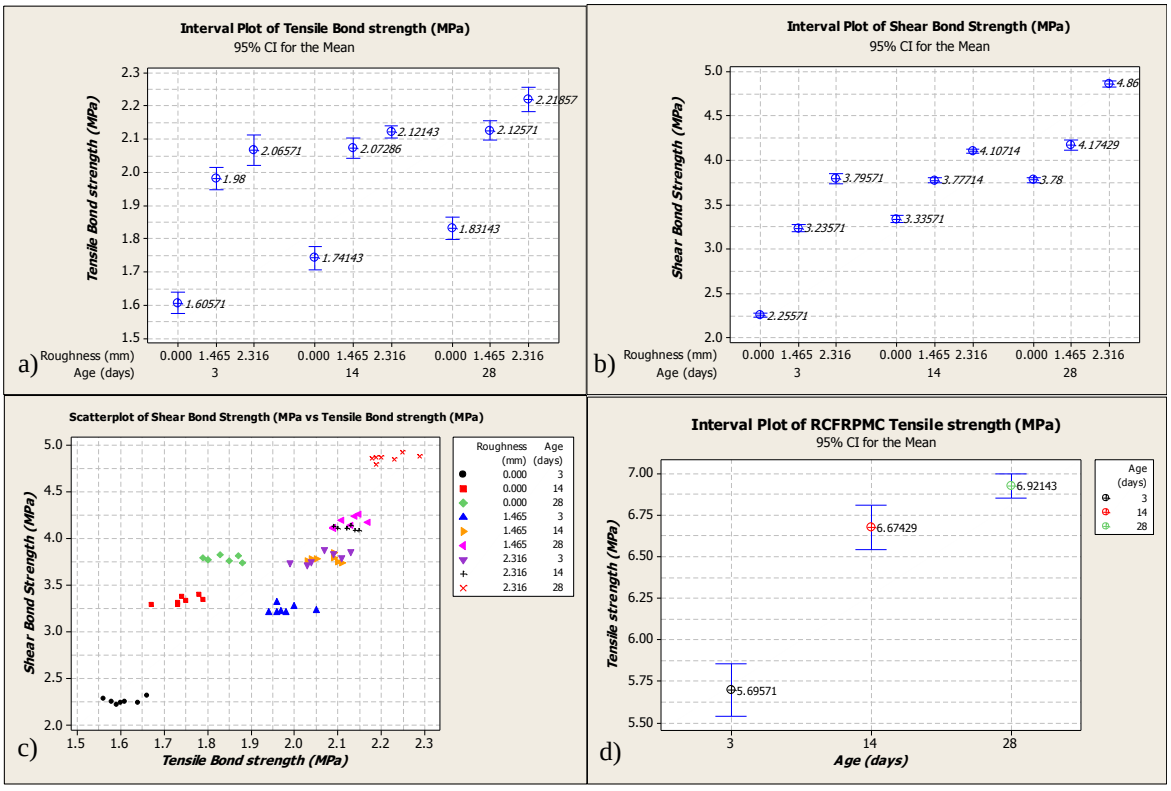

Figure 12: (a) Tensile Bond strength (b) Shear bond strength (c) Shear bond vs. Tensile Bond strength (d) Overlay BRCFRPMC Cylinder splitting (tensile) strength

cylinders from the shear test were used for density test based on the method described in ASTM D792 [27], and the percentage of air content was evaluated using equation 16 [29].

$$\sigma_{st,mod\ cub.} = \frac{2P}{\pi D}\left[(1-\gamma^2)^{5/3} - 0.0115\right] \quad (13)$$

$$\tau_{cyl.} = \frac{P}{A} \quad (14)$$

$$\sigma_{st,mod\ cyl.} = \frac{2P}{\pi D}(1-\gamma^2)^{3/2} \quad (15)$$

$$Air\ Content\ (\%) = \left(\frac{T-D}{T}\right)100 \quad (16)$$

Where, P is failure load, D is prism depth, A is cylinder cross sectional area and γ is relative width of the loading bearing strips, given by (b/D);
$b = bearing\ stripswidth$;
$T = theoretical\ air-free\ density\ (2517.3kg/m^3)$;
$D = measured\ density = 2467.7kg/m^3$.

From equation 16, the calculated air-content yields about 1.97%. This demonstrates that the optimum mixture achieves about 98.03% TAFD. These correlate well with the desirable air content and the predicted compacted density given in Table 14 and 15 respectively. In addition, the cylinder splitting tensile result for the optimum mixture illustrated in Figure 12(d) shows early high strength. The mixture attains an average tensile strength of 5.7MPa in 3 days and increases averagely by 17.8% in 25 days. In the result, it is indicative that the material can withstand significant tensile stresses before cracking during restrained drying shrinkage, if the induced strain is gradually applied.

Further, in Figure 12(a & b), interfacial tensile and shear strengths as a function of AGE and ROUGHNESS are illustrated. As seen in both cases, strength increases as each predictor increases. For specimens with $0.0mm$ texture, tensile bond increases averagely by 13.7% between age-3 and age-28; while for specimens with $1.5mm$ and $2.3mm$ textures; it increases by 7.6% and 7.3% respectively for the same age difference. The trend of shear bond strength as shown in Figure 12(b) is similar to that of tensile, though the overall contribution of surface texture appears more beneficial in shear than in tensile. This is explicable because the mechanics of interfacial de-bonding and interlocking differ in both cases. Similar observations have been argued elsewhere [45-46]. Comparatively, as shown in Figure 12(c), the estimated benefits of surface texture on shear over tensile strength range averagely between 14% and 31% for equal differential texture levels of 1.5mm and 2.3mm respectively.

4.4.1 Interfacial Bond capacity assessment

For concretes cast at different age, several codes are specific about the requirements for bond capacity. In BS EN 1504-3 [47] for instance, the tensile bond requirement for structural strengthening should be $\geq 2.0MPa$, while for non-structural work, it should exceed or be equal to $0.8MPa$. In other codes like Swedish National Road Administration (SNRA) [48], tensile bond requirements differ in values. SNRA provisions permit tensile bond capacity to be estimated using inequalities 17 [49]:

$$m \geq f_v + 1.4(s)\ \ ; x \geq 0.8\ f_v \quad (17)$$

Where,
$m = mean\ tensile\ bond\ ; s = standard\ deviation$;
$f_v = required\ tensile\ bond = 1MPa$;
$x = single\ measuring\ value$.
Thus, by checking our experimental tensile bond results against the conditions given in (17) above, the check began with the worst tensile value which is associated with the smooth interface composite tested at age 3. Here, our $m = 1.61MPa$, and $s = 0.03$, while the lowest observed value $(x) = 1.56MPa$. From here, it can be shown that:

$$1.61 \geq 1 + 1.4(0.03)$$
$$1.61 \geq 1.042\ ;\ and\ x \geq 0.8(1) \qquad (ok).$$

By inspection, referring to Figure 12(a), it would imply that all test specimens satisfied the bond criterion in this case. Hence, it can be shown at this point that the choice of a code or bond requirements for design purposes depends on the design engineer and the level of satisfaction one intends to achieve. In all, both strong chemical adhesion and sufficient degree of roughness are fundamental for enhanced tensile bond strength.

Similarly, in terms of interfacial shear capacity, codes provisions [33, 50, 51] differ in opinions and specifications. In most cases, the design shear values provided in several codes will generally be lower compared to most values obtained from the laboratory [36]. In the present work, it was observed that the shear strength values in our experiment correlate well with those found in the literature [49]; which typically fall well above $3MPa$ for 28-day bond test.

As seen in Figure 12(b), the average shear strength for smooth texture specimens is $3.8MPa$, while $1.5mm$ and $2.3mm$ texture specimens yield $4.1MPa$ and $4.9MPa$ respectively. However for design purposes, lesser values as those recommended in appropriate codes would be adopted. Usually, these design values are influenced by some long-term material response such as creep and differential length change. Besides, most of the methods for determining design bond strength in many codes do not account for the effect of different chemical bonding per se. They rely more on the interface texture and material strength parameters, which in this case does not account for any extra bond capability provided by additives like SBR polymer. No doubt that code provisions are highly conservative and generally incur huge economic implications on bonded concrete overlay construction projects.

5.0 Conclusions

From the above analyses and discussions, it is clear that mixture optimization techniques afford a flexible, quick, and economical way of modelling, designing, and selecting viable composite materials when properly calibrated with experimental data. The use of mixture screening approach as employed in this work is common when dealing with multi-component blends. The main objective of this type of approach is to screen the total components in order to identify the ones that are most important, thereby reducing the number of possible variable components. However, as occasion demands, if one intends to study the effects of each of the component for whatever reason, a factorial design may be appropriate or the current constrained mixture optimization approach can be extended accordingly to accommodate as many components as possible.

In sum, the following conclusions can be drawn:

1. The research showed that for a composite material like BRCFRPMC required to satisfy several criteria simultaneously, the use of computational statistical tools is important, considering the level of flexibility and precision required in selecting an optimum mix. Mixture experiments within the context of material modelling have been performed in executing such tasks.
2. Typically, quadratic models were fitted for the required properties, though linear models were also found adequate in some cases.
3. The overall material responses and performance were treated for typical early and matured-age of 3 and 28 days from where feasible regions of optimality were established and examined. Through optimization techniques, the optimum mixture proportion which satisfied multiple responses at the same time was selected.
4. The optimum paste mixture was found to contain about $612.9kg$ of cement, $76.2kg$ of SBR, and $123.8kg$ of WATER, per cubic meter of the total mixture.

5. The optimum consistency-time for full consolidation and composite behaviour with the substrate ordinary Portland cement concrete (OPCC) was established between 34.1 and 34.9 seconds, while the resulting apparent maximum density achieves between 97.1% - 98.0 %TAFD.
6. The optimum mixture achieved about 35.21MPa and 54.94MPa compressive strength at 3 and 28 days, with tensile strength ranging between 12.6% and 16.2% of its compressive strength.
7. The interfacial bond strength tests showed that the optimum mixture exhibited good bonding capability with the substrate OPCC both in tension and shear. The average bond strengths achieved 2.1MPa and 2.2MPa tensile and 3.8MPa and 4.9MPa shear at 0.05MPa standard deviation for early age 3-day and matured age 28-day.
8. In the bond strength tests, the results indicated that both surface texture and age had positive effects on tensile and shear strengths. Specifically, the overall contribution of surface texture appeared more beneficial in shear than in tensile. This is explicable because the mechanics of interfacial de-bonding and interlocking differ in both cases.

Acknowledgements

The authors acknowledged the financial support of Aggregate Industries, UK. Special appreciation also goes to Tarmac Ltd UK for providing materials for this research.

References

[1] Olubanwo A.O. (2013) Optimum design for Sustainable 'Green' Bonded Concrete Overlays: Failure due to shear and delamination. PhD Thesis, Department of Civil Engineering, Architecture, and Building Coventry University, United Kingdom.

[2] Ruiz, J. M., Rasmussen, R. O., Chang, G. K., Dick, J. C., Nelson, P. K., Ferragut, T. R. (2005) Computer-Based Guidelines for Concrete Pavements, Volume I—Project Summary, FHWA-HRT-04-121, Federal Highway Administration, McLean, VA 22101.

[3] ACI 211.1 (1991) Standard practice for selecting proportions for normal, heavyweight, and mass concrete. ACI Committee Report, Farmington Hills, Ml, USA.

[4] Simon, M.J (2003) Concrete Mixture Optimization Using Statistical Methods. FHWA-RD-03-060, Federal Highway Administration, Washington, DC.

[5] ACI 207.5R-99 (1999) Roller-Compacted Mass Concrete. ACI Committee Report, Farmington Hills, Ml, USA.

[6] Mehta, K.P. and Monteiro, J.M. (2006) CONCRETE: Microstructure, Properties, and Materials. 3rd edn. The McGraw - Hill Companies, Inc.

[7] ASTM C1170 / C1170M - 08 (2008) Standard Test Method for Determining Consistency and Density of Roller-Compacted Concrete Using a Vibrating Table. ASTM International, West Conshohocken, USA.

[8] ACI 325.10R-10 (2010) Report on Roller-Compacted Concrete Pavements. ACI Committee Report, Farmington Hills, Ml, USA.

[9] Casias, T. J., Goldsmith, V. D., and Benavidez, A. A. (1988) Soil Laboratory Compaction Methods Applied to RCC. In: Proceedings, Roller Compacted Concrete II, ASCE, San Diego, Calif., 107-122.

[10] Czarnecki, L., Garbacz, A., Lukowski, P., and Clifton, J.R. (1999) Optimization of Polymer Concrete Composites: Final Report. NISTIR 6361.

[11] Ohama, Y. (1995) Handbook of Polymer-Modified Concrete and Mortars. 1st edn. Noyes Publications.

[12] Czarnecki, L. and Lukowski, P. (1998) Optimization of Polymer-Cement Concrete. In: Brandt A.M. ed. Optimization methods for material design of cement-based composites E & FN Spon, London and New York, pp. 231- 250.

[13] Lin, Y., Karadelis, J.N., and Xu, Y. (2013) A new mix design method for steel fibre-reinforced, roller compacted and polymer modified bonded concrete overlays

[14] ASTM C150 – 02 (2002) Standard Specification for Portland Cement. ASTM International, West Conshohocken, USA.

[15] ACI 548.3R-03 (2003) State-of-the-Art Report on Polymer-Modified Concrete. ACI Committee Report, Farmington Hills, Ml, USA.

[16] BS EN 197-1 (2011) Cement Composition, Specifications and Conformity Criteria for common cements

[17] Simon, M.J., Lagergren, E.S., and Snyder, K.A. (1987) Concrete Mixture Optimization using Statistical Mixture Design Methods. In: Proceedings of PCI/FHWA, International Symposium on High Performance Concrete, New Orleans, Louisiana, 230 – 244.

[18] Scheffe, H. (1958) Experiments with Mixtures. Journal of Royal Statistical Society, Ser. B, 21, 344-360.

[19] McLean, R. A. and Anderson, V. L. (1966) Extreme Vertices Design of Mixture Experiments. Technometrics, 8(3) 447-454.

[20] Van Gemert, D., Czarnecki, L., Maultzsch, M., Schorn, H., Beeldens, A., Lukowski, P., & Knapen, E. (2005) Cement concrete and concrete–polymer composites: Two merging worlds: A report from 11th ICPIC Congress in Berlin, 2004. Cement and Concrete Composites, Vol. 27, No. 9-10, 926-935.

[21] ACI 548.1R-92 (1992) Guide for the Use of Polymers in Concrete. ACI Committee Report, Farmington Hills, Ml, USA.

[22] ACI 548.4-93 (1993) Standard Specification for Latex-Modified Concrete Overlays. ACI Committee Report, Farmington Hills, Ml, USA.

[23] Šušteršič, J. (2007) Overlays on Bridge Decks made from High-Performance Fibre-Reinforced Concrete.Quark Magazine, 146 – 151.

[24] Swamy, R.N. and Mangat, P.S. (1975) The onset of cracking and ductility of steel fiber concrete. Cement and Concrete Reseach, **5**, 37 – 53.

[25] Minitab 16 statistical software for Quality Improvement.

[26] ASTM C1439-99 (1999) Standard test methods for polymer-modified mortar and concrete. ASTM International, West Conshohocken, USA.

[27] National Engineering handbook (2009) Specifications for Construction Contracts, Part 642: Construction specifications 36-RCC. National Standard Construction Specifications 210-VI-NEH, United States Department of Agriculture, USA.

[28] ASTM D792 (2008) Standard Test Methods for Density and Specific Gravity (Relative Density) of Plastics by Displacement. ASTM International, West Conshohocken, USA.

[29] ASTM C138 (2001) Standard test method for density (unit weight), yield, and air content (Gravimetric). ASTM International, West Conshohocken, USA.

[30] ACI 211.3R (2002) Guide for selecting proportions for no-slump concrete. ACI Committee Report, Farmington Hills, Ml, USA.

[31] ASTM C469/C469M (1994) Standard Test Method for Static Modulus of Elasticity and Poisson's Ratio of Concrete in Compression. ASTM International, West Conshohocken, USA.

[32] VDOT (2002) Road and Bridge Specifications. Virginia Department of Transportation, Richmond

[33] Eurocode 2 (BS EN, 1992) Design of Concrete Structures.

[34] Emberson, N.K. and Mays, G.C. (1990) Significance of Property Mismatch in the Patch Repair of Structural Concrete – Part 1: Properties of Repair Systems. Magazine of Concrete Research, 42, No. 152, 147-160.

[35] Nawy, E.G. and Ukadike, M.M. (1983) Shear Transfer in Concrete and Polymer Modified Concrete Members Subjected to Shearing Loads. Journal of Testing and Evaluation, JTEVA, **11**(2), 89 – 98.

[36] Granju, J.L. (2001) Debonding of Thin Cement – Based Overlays. Journal of materials in civil engineering, 13, No. 2, 114-120.

[37] Delatte, N.J., Fowler, D.W., McCullough, B.F., and Grater, S.F. (1998) Investigating Performance of Bonded Concrete Overlays. Journal of Performance of construction facilities, 12, No. 2, 62-70.

[38] BS EN 12390-6 (2000) Testing hardened Concrete. Testing Splitting Strength of test specimens. British Standard Institute.

[39] ASTM C496 / C496M - 11 (2011) Standard Test Method for Splitting Tensile Strength of Cylindrical Concrete Specimens. ASTM International, West Conshohocken, USA.

[40] IDOT (2000). Test Method No. Iowa 406-C: Method of Test for Determining the Shearing Strength of Bonded Concrete. Iowa Department of Transportation, Ames, IA, May

[41] BS 598-3 (1985) Sampling and examination of bituminous mixtures for roads and other paved areas, Methods for design and physical testing. British Standard Institute

[42] TRRL (1969) Instructions for Using the Portable Skid Resistance Tester. Road Note 27, Transport and Road Research Laboratory HMSO.

[43] Rocco, C., Guinea, G.V., Planas, J. and Elice, M. (2001) Review of the splitting-test standards from a fracture mechanics point of view. Cement and Concrete Research, 31, 73 – 82.

[44] Tang, T. (1994) Effect of load-distributed width in split tension of un-notched and notched cylindrical specimens. Journal of Testing and Evaluation, **22**(5) 401 – 409.

[45] Beushausen, H.D. (2005) Long-Term Performance of Bonded Overlays Subjected to Differential Shrinkage. PhD Thesis, University of Cape Town, South Africa.

[46] Benoît Bissonnette, Alexander M. Vaysburd, and Kurt F. von Fay (2012) Best Practices for Preparing Concrete Surfaces Prior to Repairs and Overlays - Report Number MERL 12-17. U.S. Department of the Interior Bureau of Reclamation Technical Service Center Denver, Colorado

[47] BS EN 1504-3 (2005) Products and systems for the protection and repair of concrete structures. Definitions, requirements, quality control and evaluation of conformity. Structural and non-structural repair. British Standard Institute.

[48] Swedish National Road Administration (SNRA) (2004) General Technical Regulations for Bridges. Publication No. 2004:56, Borlange, Sweden.

[49] Silfwerbrand, J. Beushausen, H. and Courard, L. (2012) Bond. In: Bissonnette, B., Courard, L., Fowler, D.W., and Granju, J. ed. State-of-the-Art Report of the RILEM Technical Committee 193-RLS, Springer, 51-79.

[50] ACI 318 – 05 (2005) Building Code Requirements for Structural Concrete and Commentary. American Concrete Institute, Farmington Hills, Ml, USA.

[51] CEB-FIP-90 (1993) Model code for Concrete Structures, 1st edn. Thomas Telford